PFC/JA-80-9

TEARING-MODE STABILITY PROPERTIES OF A FIELD-REVERSED ION LAYER AT MARGINAL STABILITY

James Chen

and

Ronald C. Davidson

March, 1980

PFC/JA-80-9

TEARING-MODE STABILITY PROPERTIES OF A FIELD-REVERSED ION LAYER AT MARGINAL STABILITY

James Chen
Plasma Fusion Center
Massachusetts Institute of Technology, Cambridge, Mass., 02139

Ronald C. Davidson†
Plasma Research Institute
Science Applications Inc., Boulder, Colorado 80302

Tearing-mode stability properties are investigated at marginal stability ($\omega=0$) for a rotating, nonrelativistic cylindrically symmetric ion layer immersed in an axial magnetic field $B_z^0(r)\hat{e}_z = [B_0+B_z^s(r)]\hat{e}_z$. The analysis is carried out within the framework of a Vlasov-fluid model in which the electrons are described as a macroscopic, cold fluid, and the layer ions are described by the Vlasov equation. Tearing-mode stability properties are calculated numerically for azimuthally symmetric perturbations about an ion layer equilbrium described by f_i^0=const $\times \exp[-(H+\omega_\theta P_\theta)/T]$. Here, H is the energy, P_θ is the canonical angular momentum, T=const is the temperature, $-\omega_\theta$=const is the angular velocity of mean rotation, and the density profile is $n(r)=n_0 \mathrm{sech}^2(r^2/2\delta^2 - r_0^2/2\delta^2)$, where $\delta^4=2c^2T/(m_i\omega_\theta^2\omega_{pi}^2)$ and $\omega_{pi}^2=4\pi n_0 e^2/m_i$. The marginal stability eigenvalue equation for the perturbation amplitude $\hat{A}_\theta(r)$ has the form of a Schroedinger equation, with "energy" eigenvalue $k_z^2\delta^2$ and effective potential $V(r)=\delta^2/r^2-2(r^2/\delta^2)\mathrm{sech}^2(r^2/2\delta^2-r_0^2/2\delta^2)$. This equation is solved numerically for $\hat{A}_\theta(r)$ and the normalized axial wave number at marginal stability (denoted by $k_0^2\delta^2$) as a function of normalized layer radius r_0/δ and magnetic field depression $\beta_i^{-1/2}$ $[B_0-B_z^0(r=0)]/B_0$, where $\beta_i=8\pi n_0 T/B_0^2$. For $r_0^2/\delta^2 > 1$, the numerical analysis shows that $k_0^2\delta^2$ can be approximated by $k_0^2\delta^2=r_0^2/\delta^2$ to a high degree of accuracy.

† Permanent Address: Plasma Fusion Center, Massachusetts Institute of Technology, Cambridge, Mass., 02139

I. INTRODUCTION

There is considerable interest in the basic equilibrium, stability and transport properties of intense ion beams in a background plasma. As a result of recent technological advances in the generation of intense ion beams, such beams have a variety of possible applications, including (a) the production of field-reversed configurations for magnetic fusion applications [1-9], (b) applications to light ion[10-14] and heavy ion[15,16] fusion, and (c) the development of novel techniques for focussing intense ion beams.[17] In this paper, we investigate the tearing-mode stability properties at marginal stability (ω=0) for a rotating, nonrelativistic, cylindrically symmetric ion layer immersed in an axial magnetic field $B_z^0(r)\hat{e}_z = [B_0+B_z^s(r)]\hat{e}_z$. The analysis is carried out within the framework of a hybrid (Vlasov-fluid) model[18] in which the electrons are described as a macroscopic, cold fluid, and the layer ions are described by the Vlasov equation. Unlike previous detailed analyses[9] of the tearing-mode instability, no a priori assumption is made that the radial thickness (δ) of the layer is small in comparison with the mean radius (r_0). Moreoever, the numerical analysis is carried out with full cylindrical effects, and not within the context of the slab approximation.[7]

Tearing-mode stability properties are calculated for the specific choice of ion beam distribution function [Eq. (21)] corresponding to thermal equilibrium,

$$f_i^0(H+\omega_\theta P_\theta) = \frac{n_o}{(2\pi T/m_i)^{3/2}} \times \exp[-(H+\omega_\theta P_\theta)/T] ,$$

where H is the energy, P_θ is the canonical angular momentum, T=const is the temperature, n_0=const is the maximum density, and $-\omega_\theta$=const is the angular velocity of mean rotation. The density profile corresponding to Eq. (21) is [Eq. (22)]

$$n(r)=n_0 \operatorname{sech}^2\left(\frac{r^2-r_0^2}{2\delta^2}\right) ,$$

where r_0^2=const, $\delta^4=2c^2T/(m_i\omega_\theta^2\omega_{pi}^2)$ and $\omega_{pi}^2=4\pi n_0 e^2/m_i$. In the present analysis, we assume that the net current carried by the background electrons is equal to zero, so that the magnetic self field $B_z^s(r)$ is generated entirely by the mean rotational motion of the ions.

The stability analysis assumes azimuthally symmetric perturbations ($\partial/\partial\theta=0$) of the form $\delta\psi(\underset{\sim}{x},t)=\hat{\psi}(r)\exp(ik_z z-i\omega t)$. For the choice of equilibrium distribution function in Eq. (21), the marginal stability (ω=0) eigenvalue equation (28) has been solved numerically for a broad range of equilibrium parameters. In particular, Equation (28) has the form of a Schroedinger equation for the perturbation amplitude $\hat{A}_\theta(r)$, with "energy" eigenvalue $k^2=k_z^2\delta^2$ and effective potential $V(R)=R^{-2} -2R^2\operatorname{sech}^2(R^2/2-R_0^2/2)$, where $R=r/\delta$ and $R_0=r_0/\delta$. In Sec. III, Eq. (28) is solved numerically for both the eigenfunction $\hat{A}_\theta(R)$ and the eigenvalue (denoted by $k_0^2\delta^2$) as a function of normalized layer radius r_0/δ and normalized magnetic field depression $\beta_i^{-1/2}[B_0-B_z^0(r=0)]/B_0$, where $\beta_i=8\pi n_0T/B_0^2$. This procedure determines the critical axial wavenumber k_0 corresponding to marginal stability (Imω=0). In particular, purely growing (and purely damped) solutions exist for axial wavenumber k_z in the range $0 < k_z^2 < k_0^2$. On the other hand, Imω=0 for $k_z^2 \geq k_0^2$ and Reω is generally non-zero. For $r_0^2/\delta^2 > 1$, the numerical analysis shows that $k_0^2\delta^2$ can be approximated by [Eq. (32)]

$$k_0^2\delta^2 = \frac{r_0^2}{\delta^2}$$

to a high degree of accuracy. .

The organization of this paper is the following. In Sec. II, we obtain the eigenvalue equation (16) [or, equivalently, Eq. (20)] valid at marginal stability for the general class of rigid-rotor ion equilibria $f_i^0(H+\omega_\theta P_\theta)$. In Sec. III, marginal stability properties are calculated in detail for the choice of thermal equilibrium distribution in Eq. (21).

II. THEORETICAL MODEL AND GENERAL STABILITY ANALYSIS

The present analysis is carried out for perturbation frequencies ω satisfying $|\omega| \lesssim \omega_{ci}$, where $\omega_{ci}=eB_0/m_ic$ is the ion cyclotron frequency associated with the externally applied field B_0. In this regard, charge neutrality is assumed to first order, and the displacement current is neglected in the $\nabla \times \delta\mathbf{B}$ Maxwell equation. It is also assumed that the equilibrium radial electric field is equal to zero ($E_r^0=0$), which is consistent with local equilibrium charge neutrality, $n_e^0(r)=n_i^0(r)\equiv n(r)$. To further simplify the analysis, we assume that all of the equilibrium current is carried by the layer ions, and that the mean equilibrium flow velocity of the electrons is equal to zero ($\mathbf{V}_e^0=0$). Moreover, under typical experimental conditions, the thermal ion gyroradius can be comparable in size to the layer radius. Thus, in the present analysis, the layer ions are described by the Vlasov equation, and the electrons are described as a macroscopic cold fluid. Such a hybrid model[18] has proved useful in describing the equilibrium and stability properties for a variety of field-reversed configurations[9] and linear fusion systems.[19]

In the stability analysis, we consider azimuthally symmetric perturbations characterized by $\partial/\partial\theta=0$. Using the method of characteristics, the linearized Vlasov equation for the ions can be integrated to give

$$\delta f_i(\mathbf{x},\mathbf{v},t)=-\frac{e}{m_i}\int_{-\infty}^{t}dt'\left(\delta\mathbf{E}(\mathbf{x}',t')+\frac{\mathbf{v}'\times\delta\mathbf{B}(\mathbf{x}',t')}{c}\right)\cdot\frac{\partial}{\partial\mathbf{v}'}f_i^0(\mathbf{x}',\mathbf{v}') \ , \tag{1}$$

where the particle trajectories $(\mathbf{x}',\mathbf{v}')$ satisfy $d\mathbf{x}'/dt'=\mathbf{v}'$ and $d\mathbf{v}'/dt'=e\mathbf{v}'\times B_z^0(r')\hat{\mathbf{e}}_z/m_ic$, with initial conditions $\mathbf{x}'(t'=t)=\mathbf{x}$ and $\mathbf{v}'(t'=t)=\mathbf{v}$. In Eq. (1), $f_i^0(\mathbf{x}',\mathbf{v}')=f_i^0(H+\omega_\theta P_\theta)$ is a function of the single-particle constants of the motion (H,P_θ) in the equilibrium field configuration. Here, $H=(m_i/2)(v_r^2+v_\theta^2+v_z^2)$ is the kinetic energy, and $P_\theta=m_i rv_\theta+(e/c)rA_\theta^0(r)$ is the canonical angular momentum. Moreover, +e is the ion charge, m_i is the ion mass, $-\omega_\theta=r^{-1}(\int d^3v\ v_\theta f_i^0)/(\int d^3v\ f_i^0)=\text{const}$ is the mean angular velocity of the layer ions, and the equilibrium axial magnetic field $B_z^0(r)$ is related to the equilibrium vector potential $A_\theta^0(r)$ by $B_z^0(r)=r^{-1}(\partial/\partial r)(rA_\theta^0)$. The axial magnetic field $B_z^0(r)$ is determined self-consistently from $\partial B_z^0/\partial r=(4\pi e/c)\omega_b rn(r)$, where the equilibrium ion density $n_i^0(r)\equiv n(r)$ is defined by

$$n(r)=\int d^3v\ f_i^0(H+\omega_\theta P_\theta)\ . \tag{2}$$

The linearized continuity and momentum transfer equations for the cold fluid electrons can be expressed as

$$\frac{\partial}{\partial t}\,\delta n_e+\nabla\cdot(n\delta\underset{\sim}{V}_e)=0\ , \tag{3}$$

and

$$m_e\,\frac{\partial}{\partial t}\,\delta\underset{\sim}{V}_e=-e\left(\delta\underset{\sim}{E}+\frac{\delta\underset{\sim}{V}_e\times B_z^0\hat{\underset{\sim}{e}}_z}{c}\right)\ , \tag{4}$$

where $\delta n_e(\underset{\sim}{x},t)$ is the perturbed electron density and $\delta\underset{\sim}{V}_e(\underset{\sim}{x},t)$ is the perturbed electron fluid velocity. Within the context of the assumptions enumerated in the previous paragraph, the perturbed electric and magnetic fields, $\delta\underset{\sim}{E}(\underset{\sim}{x},t)$ and $\delta\underset{\sim}{B}(\underset{\sim}{x},t)$, are determined self-consistently from the Maxwell equations

$$\nabla\times\delta\underset{\sim}{E}=-\frac{1}{c}\frac{\partial}{\partial t}\,\delta\underset{\sim}{B}\ , \tag{5}$$

$$\nabla\times\delta\underset{\sim}{B}=\frac{4\pi}{c}\,e\int d^3v\ \underset{\sim}{v}\ \delta f_i(\underset{\sim}{x},\underset{\sim}{v},t)-\frac{4\pi e}{c}\,n\delta\underset{\sim}{V}_e(\underset{\sim}{x},t)\ , \tag{6}$$

and

$$\delta n_i(\underset{\sim}{x},t)=\delta n_e(\underset{\sim}{x},t)\ , \tag{7}$$

where $\nabla\cdot\delta\mathbf{B}=0$, and $\delta n_i(\mathbf{x},t)=\int d^3v\ \delta f_i(\mathbf{x},\mathbf{v},t)$ is the perturbed ion density. Consistent with first-order charge neutrality [Eq. (7)], we choose a gauge in which the perturbed electric and magnetic fields are expressed as $\delta\mathbf{E}(\mathbf{x},t)=-c^{-1}(\partial/\partial t)\delta\mathbf{A}(\mathbf{x},t)$ and $\delta\mathbf{B}(\mathbf{x},t)=\nabla\times\delta\mathbf{A}(\mathbf{x},t)$, with $\nabla\cdot\delta\mathbf{A}=0$.

It is convenient to introduce the Lagrangian displacement vector $\boldsymbol{\xi}(\mathbf{x},t)$ defined by

$$\delta\mathbf{V}_e(\mathbf{x},t)=\frac{\partial}{\partial t}\boldsymbol{\xi}(\mathbf{x},t)\ . \tag{8}$$

Substituting Eq. (8) into Eq. (4) and integrating with respect to t, we find

$$\delta\mathbf{A}(\mathbf{x},t)=\left(\frac{m_e c}{e}\right)\frac{\partial}{\partial t}\boldsymbol{\xi}+\boldsymbol{\xi}\times\mathbf{B}^0\ , \tag{9}$$

where $\mathbf{B}^0=B_z^0(r)\hat{\mathbf{e}}_z$. Moreover, integrating Eq. (3) with respect to t gives

$$\delta n_e(\mathbf{x},t)=-\nabla\cdot[n(r)\boldsymbol{\xi}(\mathbf{x},t)]\ , \tag{10}$$

for the perturbed electron density.

In the subsequent analysis, it is assumed that all perturbed quantities vary according to $\delta\psi(\mathbf{x},t)=\hat{\psi}(r)\exp(ik_z z-i\omega t)$, where ω is the complex oscillation frequency, and k_z is the (real) axial wavenumber of the perturbation. Moreover, we examine the class of purely growing modes with $\mathrm{Re}\omega=0$, and consider the state corresponding to marginal stability with $\mathrm{Im}\omega=0$. Imposing the condition

$$\omega=0, \tag{11}$$

and assuming azimuthally symmetric perturbations $(\partial/\partial\theta=0)$, then $\nabla\cdot\hat{\mathbf{A}}=0$ and $\hat{\mathbf{A}}=\hat{\boldsymbol{\xi}}\times\mathbf{B}^0$ [Eq. (9)] can be combined to give

$$\hat{A}_r(r)=\hat{A}_z(r)=0 \ ,$$

$$\hat{\xi}_\theta(r)=0 \ , \tag{12}$$

$$\hat{\xi}_r(r)=-\hat{A}_\theta(r)/B_z^0(r) \ ,$$

at marginal stability. Moreover, making use of $\delta\underset{\sim}{B}=\nabla\times\delta\underset{\sim}{A}$ and Eq. (12), we find

$$\hat{B}_r(r)=-ik_z\hat{A}_\theta(r) \ ,$$

$$\hat{B}_\theta(r)=0 \ , \tag{13}$$

$$\hat{B}_z(r)=\frac{1}{r}\frac{\partial}{\partial r}\,[r\hat{A}_\theta(r)] \ .$$

In addition, the perturbed electric field is $\delta\underset{\sim}{E}=i(\omega/c)\delta\underset{\sim}{A}=0$ for $\omega=0$. In order to evaluate the perturbed ion distribution function δf_i [Eq. (1)], we note from Eq. (13) that $\underset{\sim}{v}\times\underset{\sim}{\hat{B}}\cdot(\partial/\partial\underset{\sim}{v})f_i^0(H+\omega_\theta P_\theta)=(m_i r\omega_\theta)(\partial f_i^0/\partial H)$ $\underset{\sim}{v}\times\underset{\sim}{\hat{B}}\cdot\underset{\sim}{\hat{e}}_\theta=-m_i\omega_\theta(\partial f_i^0/\partial H)[ik_z v_z r\hat{A}_\theta+v_r(\partial/\partial r)(r\hat{A}_\theta)]$. Defining $\delta f_i(\underset{\sim}{x},\underset{\sim}{v},t)=\hat{f}_i(r,\underset{\sim}{v})\exp(ik_z z-i\omega t)$, Eq. (1) then gives

$$\hat{f}_i(r,\underset{\sim}{v})=\frac{e\omega_\theta}{c}\frac{\partial f_i^0}{\partial H}\int_{-\infty}^{t}dt'\exp[ik_z(z'-z)]$$
$$\times\left\{ik_z v_z' r'\hat{A}_\theta(r')+v_r'\frac{\partial}{\partial r'}\,[r'\hat{A}_\theta(r')]\right\} \ , \tag{14}$$

at marginal stability ($\omega=0$). The integrand in Eq. (14) can also be expressed as $(d/dt')\{r'\hat{A}_\theta(r')\exp[ik_z(z'-z)]\}=\underset{\sim}{v}'\cdot\underset{\sim}{\nabla}'\{r'\hat{A}_\theta(r')\exp[ik_z(z'-z)]\}$ for $\omega=0$. Integrating with respect to t', Eq. (14) gives

$$\hat{f}_i(r,\underset{\sim}{v})=\frac{e\omega_\theta}{c}\,r\hat{A}_\theta(r)\,\frac{\partial f_i^0}{\partial H} \ , \tag{15}$$

where use has been made of $\underset{\sim}{x}'(t'=t)=\underset{\sim}{x}$. Introducing the perturbed flux function $\hat{\psi}(r)=r\hat{A}_\theta(r)$ and making use of Eq. (15), the perturbed Maxwell equation (6) can be expressed as

$$r\frac{\partial}{\partial r}\left(\frac{1}{r}\frac{\partial}{\partial r}\hat{\psi}\right)-k_z^2\hat{\psi}+\frac{4\pi e^2\omega_\theta r}{c^2}\left(\int d^3v\ v_\theta\frac{\partial f_i^0}{\partial H}\right)\hat{\psi}=0\ , \tag{16}$$

with boundary conditions $\hat{\psi}(r=0)=0$ and $\lim_{r\to\infty}[r^{-1}(\partial/\partial r)\hat{\psi}(r)]=0$. Moreover, from Eqs. (7), (10), and (15), the quasineutrality condition $\hat{n}_e(r)=\hat{n}_i(r)$ can be expressed as

$$ik_z n\hat{\xi}_z-\frac{1}{r}\frac{\partial}{\partial r}[n(\hat{\psi}/B_z^0)]=-e\omega_\theta\hat{\psi}\left[\int d^3v(\partial f_i^0/\partial H)\right]\ , \tag{17}$$

where $n(r)=\int d^3v\ f_i^0$ is the equilibrium density profile and $B_z^0(r)$ is the equilibrium axial magnetic field.

The eigenvalue equations (16) and (17) are valid at marginal stability ($\omega=0$) for the general class of rigid rotor ion equilibria $f_i^0(H+\omega_\theta P_\theta)$. Moreover, as a procedural point, Eq. (16) can be used to determine the eigenfunction $\hat{\psi}(r)$. Equation (17) can then be used to determine the corresponding axial displacement $\hat{\xi}_z(r)$ self-consistently. Before examining Eq. (16) for a specific choice of ion distribution function f_i^0, it is useful to derive some equilibrium identities valid for general $f_i^0(H+\omega_\theta P_\theta)$. First, noting that $H+\omega_\theta P_\theta=(m_i/2)\times[v_r^2+(v_\theta+\omega_\theta r)^2+v_z^2]-(m_i/2)\omega_\theta^2r^2+(e/c)(\omega_\theta r)A_\theta^0$, it follows that

$$\int d^3v\ v_\theta\frac{\partial f_i^0}{\partial H}=-\omega_\theta r\int d^3v\frac{\partial f_i^0}{\partial H}\ . \tag{18}$$

Second, making use of $n(r)=\int d^3v\ f_i^0(H+\omega_\theta P_\theta)$ and $B_z^0(r)=r^{-1}(\partial/\partial r)(rA_\theta^0)$, it is straightforward to show that

$$\frac{\partial}{\partial r}n(r)=-m_i\omega_\theta r\left(\omega_\theta-\frac{eB_z^0(r)}{m_ic}\right)\int d^3v\frac{\partial f_i^0}{\partial H}\ . \tag{19}$$

Substituting Eqs. (18) and (19) into Eq. (16), the marginal stability eigenvalue equation for the perturbed flux function $\hat{\psi}(r)=r\hat{A}_\theta(r)$ can be expressed in the equivalent form

$$r\frac{\partial}{\partial r}\left(\frac{1}{r}\frac{\partial}{\partial r}\hat{\psi}\right)-k_z^2\hat{\psi}+\frac{4\pi e^2}{m_i c^2}\frac{\omega_\theta r\partial n(r)/\partial r}{\omega_\theta-eB_z^0(r)/m_i c}\hat{\psi}=0\ , \tag{20}$$

which is valid for the general class of rigid-rotor ion equilibria $f_i^0(H+\omega_\theta P_\theta)$.

III. STABILITY PROPERTIES FOR GIBBS ION EQUILIBRIUM

In this section, we specialize to the case where f_i^0 corresponds to the Gibbs equilibrium

$$f_i^0 = \frac{n_0}{(2\pi T/m_i)^{3/2}} \exp\left[-\frac{1}{T}(H+\omega_\theta P_\theta)\right] , \qquad (21)$$

where n_0=const, and T=const is the (uniform) ion temperature. From $n(r)=\int d^3v f_i^0$ and $\partial B_z^0/\partial r=(4\pi e/c)\omega_\theta r n(r)$, the equilibrium density and magnetic field profiles are given by the well-known expressions[6-8]

$$n(r)=n_0 \mathrm{sech}^2\left(\frac{r^2-r_0^2}{2\delta^2}\right) , \qquad (22)$$

and

$$B_z^0(r)= \frac{cT}{e\omega_\theta}\left[\frac{m_i\omega_\theta^2}{T} + \frac{2}{\delta^2}\tanh\left(\frac{r^2-r_0^2}{2\delta^2}\right)\right] , \qquad (23)$$

where $\delta^4=2c^2T/(m_i\omega_\theta^2\omega_{pi}^2)$, $\omega_{pi}^2=4\pi n_0 e^2/m_i$, and r_0^2=const. Note from Eq. (22) that n_0 corresponds to the maximum ion density, which occurs at $r=r_0$. We denote the externally applied magnetic field by $B_0=B_z^0(r\to\infty)$ and assume $B_0 > 0$ without loss of generality. It follows from Eq. (23) that the equilibrium exists only for $\omega_\theta > 0$. Moreover, B_0 is related to other equilibrium parameters by

$$\frac{eB_0}{m_i c}\omega_\theta=\omega_\theta^2+v_i^2/\delta^2 , \qquad (24)$$

where $v_i=(2T/m_i)^{1/2}$ is the ion thermal speed, and $v_i^2/\delta^2=(v_i/c)\omega_\theta\omega_{pi}$. Evaluating Eq. (23) at r=0 gives

$$\frac{eB_z^0(0)}{m_i c}\omega_\theta=\omega_\theta^2-\frac{v_i^2}{\delta^2}\tanh\frac{r_0^2}{2\delta^2} . \qquad (25)$$

Subtracting Eq. (25) from Eq. (24), the fractional magnetic field depression can be expressed as[8]

$$\frac{B_0-B_z(0)}{B_0}=\beta_i^{1/2}\left[1+\tanh(r_0^2/2\delta^2)\right] , \qquad (26)$$

where $\beta_i=8\pi n_0T/B_0^2$ is the ratio of ion pressure (n_0T) at $r=r_0$ to magnetic pressure $(B_0^2/8\pi)$ as $r\to\infty$. Equation (26) is a useful identity relating the normalized layer radius (r_0/δ) to β_i and $[B_0-B_z(0)]/B_0$.

To analyze the marginal eigenvalue equation (16), it is convenient to introduce the dimensionless quantities

$$R=r/\delta \ , \quad R_0=r_0/\delta \ , \quad k^2=k_z^2\delta^2 \ . \tag{27}$$

Substituting Eqs. (18), (21), and (22) into Eq. (16), the eigenvalue equation for $\hat{\psi}=r\hat{A}_\theta$ can be expressed in the form of a Schroedinger equation for $\hat{A}_\theta$, i.e.,

$$\frac{1}{R}\frac{\partial}{\partial R}R\frac{\partial}{\partial R}\hat{A}_\theta+\left(-k^2-\frac{1}{R^2}+2R^2\mathrm{sech}^2\left(\frac{R^2-R_0^2}{2}\right)\right)\hat{A}_\theta=0 \ , \tag{28}$$

with boundary conditions $[R\hat{A}_\theta]_{R=0}=0$ and $\lim_{R\to\infty}[R^{-1}(\partial/\partial R)(R\hat{A}_\theta)]=0$. From Eq. (28), $-k^2=E$ plays the role of the energy eigenvalue, and the effective potential in cylindrical coordinates is

$$V(R)=\frac{1}{R^2}-2R^2\mathrm{sech}^2\left(\frac{R^2-R_0^2}{2}\right) \tag{29}$$

Near the origin $(R^2 \ll k^2)$, the solution to Eq. (28) can be approximated by

$$R\hat{A}_\theta=ARI_1[(k^2R^2)^{1/2}] \ , \tag{30}$$

where A is a constant coefficient, and $I_1(x)$ is the modified Bessel function of the first kind of order unity. On the other hand, for $R \gg R_0$, the asymptotic solution to Eq. (28) is given by

$$R\hat{A}_\theta\simeq B\sqrt{\pi/2}(R^2/k^2)^{1/4}\exp[-(k^2R^2)^{1/2}] \ , \tag{31}$$

where B is a constant.

The effective potential V(R) [Eq. (29)] is illustrated in Fig. 1 for $R_0=r_0/\delta= 3$. Note that the eigenvalue equation (28) not only determines the eigenfunction $\hat{A}_\theta(R)$ at marginal stability but also determines the discrete (quantized) value of normalized axial wavenumber-squared (denote by $k^2 \equiv k_0^2\delta^2$) corresponding to $\mathrm{Im}\omega=0$.

The eigenvalue equation (28) has been solved numerically for R_0^2 in the range $0 \leq R_0^2 < 10$. For each value of R_0^2, it is found that there is only one allowed value of $k_0^2\delta^2$, corresponding to a single bound energy eigenstate. The numerical results are summarized in Fig. 2, where the eigenvalue $k_0^2\delta^2$ is plotted as a function of R_0^2. The same information is presented in Fig. 3, where Eq. (26) and the information in Fig.2 are used to plot $k_0^2\delta^2$ versus the normalized magnetic field depression $\beta_i^{-1/2}[B_0-B_z^0(0)]/B_0$. The universal curves in Figs. 2 and 3 determine the critical wavenumber $k_0^2\delta^2$ corresponding to marginal stability ($\mathrm{Im}\omega=0$). In particular, purely growing (and purely damped) solutions exist for axial wavenumber k_z in the range $0 < k_z^2 < k_0^2$. On the other hand, $\mathrm{Im}\omega=0$ for $k_z^2 \geq k_0^2$, and $\mathrm{Re}\omega$ is generally non-zero. Figures 4 and 5 illustrate the equilibrium profiles n(r) [Eq. (22)] and $B_z^0(r)$ [Eq. (23)] and the eigenfunction $r\hat{A}_\theta(r)$ at marginal stability [Eq. (28)] for the two cases $r_0/\delta= 1$ [Fig. 4] and $r_0/\delta= 3$ [Fig. 5], and for $\beta_i = 1$ (maximum field depression). We note from Figs. 4 and 5 that the eigenfunction $rA_\theta(r)$ does not become localized about $r \approx r_0$ for $r_0/\delta >> 1$, although V(R) is strongly peaked for $r_0/\delta >> 1$ [Fig. 1]. We also note from Figure 2, that $k_0^2\delta^2$ can be approximated by

$$k_0^2\delta^2 = \frac{r_0^2}{\delta^2}$$

to a high degree of accuracy, for $r_0^2/\delta^2 > 1$.

IV. CONCLUSIONS

In this paper, we have investigated the tearing-mode stability properties at marginal stability ($\omega=0$) for a rotating, nonrelativistic, cylindrically symmetric ion layer immersed in an axial magnetic field $B_z^0(r)\hat{e}_z$. In Sec. II, we derived the eigenvalue equation (16) [or, equivalently, Eq. (20)] valid at marginal stability for azimuthally symmetric ($\partial/\partial\theta=0$) perturbations about the general class of rigid-rotor ion equilibria $f_i^0(H+\omega_\theta P_\theta)$. In Sec. III, marginal stability properties were calculated in detail for the choice of thermal equilibrium distribution in Eq. (21).

For the choice of thermal equilibrium distribution function in Eq. (21), the marginal stability ($\omega=0$) eigenvalue equation (28) has been solved numerically for a broad range of equilibrium parameters. In particular, Eq. (28) has the form of a Schroedinger equation for the perturbation amplitude $\hat{A}_\theta(R)$, with "energy" eigenvalue $k^2=k_z^2\delta^2$ and effective potential $V(R)=R^{-2}-2R^2\ \mathrm{sech}^2(R^2/2-R_0^2/2)$, where $R=r/\delta$ and $R_0=r_0/\delta$. In Sec. III, Eq. (28) was solved numerically for both the eigenfunction $\hat{A}_\theta(R)$ and the eigenvalue (denoted by $k_0^2\delta^2$) as a function of normalized layer radius r_0/δ [Fig. 2] and normalized magnetic field depression $\beta_i^{-1/2}[B_0-B_z^0(r=0)]/B_0$ [Fig. 3] where $\beta_i=8\pi n_0T/B_0^2$.

This procedure determines the critical axial wavenumber k_0 corresponding to marginal stability ($\mathrm{Im}\,\omega=0$). In particular, purely growing (and purely damped) solutions exist for axial wavenumber k_z

in the range $0 < k_z^2 < k_0^2$. On the other hand, Imω=0 for $k_z^2 \geq k_0^2$ and Reω is generally non-zero. For $r_0^2/\delta^2 > 1$, the numerical analysis shows that $k_0^2\delta^2$ can be approximated by [Eq. (32)]

$$k_0^2\delta^2 = \frac{r_0^2}{\delta^2}$$

to a high degree of accuracy.

ACKNOWLEDGMENTS

This research was supported in part by the Office of Naval Research and in part by the National Science Foundation.

FIGURE CAPTIONS

Fig. 1 Plot of effective potential $V(R)$ versus $R=r/\delta$, for $r_0/\delta=1$ and $r_0/\delta=3$

Fig. 2 Normalized critical wavenumber $k_0^2\delta^2$ [Eq. (28)] plotted versus r_0^2/δ^2 .

Fig. 3 Normalized critical wavenumber $k_0^2\delta^2$ [Eq. (28)] plotted versus $\beta_i^{-1/2}[B_0-B_z^0(0)]/B_0$.

Fig. 4 Plot of (a) $n(r)/n_0$ [Eq. (22)], (b) $B_z^0(r)/B_0$ [Eq. (23)], and (c) $r\hat{A}_\theta(r)$ [Eq. (28)] versus r/δ for $r_0/\delta=1.0$, $\beta_i=1.0$ and $k_0^2\delta^2=0.68$.

Fig. 5 Plot of (a) $n(r)/n_0$ [Eq. (22)], (b) $B_z^0(r)/B_0$ [Eq. (23)], and (c) $r\hat{A}_\theta(r)$ [Eq. (28)] versus r/δ for $r_0/\delta=3.0$, $\beta_i=1.0$ and $k_0^2\delta^2=8.95$

REFERENCES

1. C.A. Kapetanakos, J. Golden, J.A. Pasour, S.J. Marsh, and R.A. Mahaffey, Phys. Rev. Lett., to be published (1980).
2. S.J. Marsh, A.T. Drobot, J. Golden, and C.A. Kapetanakos, Phys. Fluids 21, 1045 (1978).
3. R.N. Sudan and E. Ott, Phys. Rev. Lett. 33, 355 (1974).
4. H.H. Fleischmann and T. Kammash, Nucl. Fusion 15, 1143 (1975).
5. C.A. Kapetanakos, J. Golden, and K.R. Chu, Plasma Phys. 19, 387 (1977).
6. K.D. Marx, Phys. Fluids 11, 357 (1968).
7. J.P. Freidberg and R.L. Morse, Phys. Fluids 12, 887 (1969).
8. J. Chen and R.C. Davidson, Phys. Fluids 23, 302 (1980).
9. H.S. Uhm and R.C. Davidson, Phys. Fluids 23, 348 (1980).
10. R.N. Sudan, Phys. Rev. Lett. 41, 476 (1978).
11. S.A. Goldstein, D.P. Bacon, D. Mosher, and G. Cooperstein, in Proceedings of the 2nd International Topical Conference on High Power Electron and Ion Beam Research and Technology (Cornell University, Ithaca, New York, 1977), Vol. I,p. 71; R.L. Martin, ibid., Vol. 1, p. 113.
12. M.J. Clauser, Phys. Rev. Lett. 35 848 (1975).
13. J.W. Shearer, Nucl. Fusion 15, 952 (1975).
14. S. Humphries, R.N. Sudan, and L. Wiley, J. Appl. Phys. 47, 2382 (1976).
15. A.W. Maschke, IEEE Trans. Nucl. Sci. 22, 1825 (1975).
16. R. Burke, Y. Cho, J. Fasolo, S. Fenster, M. Fors, T. Khoe, A. Langsdorf, and R. Martin, IEEE Trans. Nucl. Sci. NS-24, 1012 (1977).
17. F. Winterberg, Phys. Rev. Lett. 37, 713 (1976).

18. J.P. Freidberg, Phys. Fluids 15, 1102 (1972).

19. R.C. Davidson, H.S. Uhm and R. Aamodt, Phys. Fluids 22, 2158 (1979).

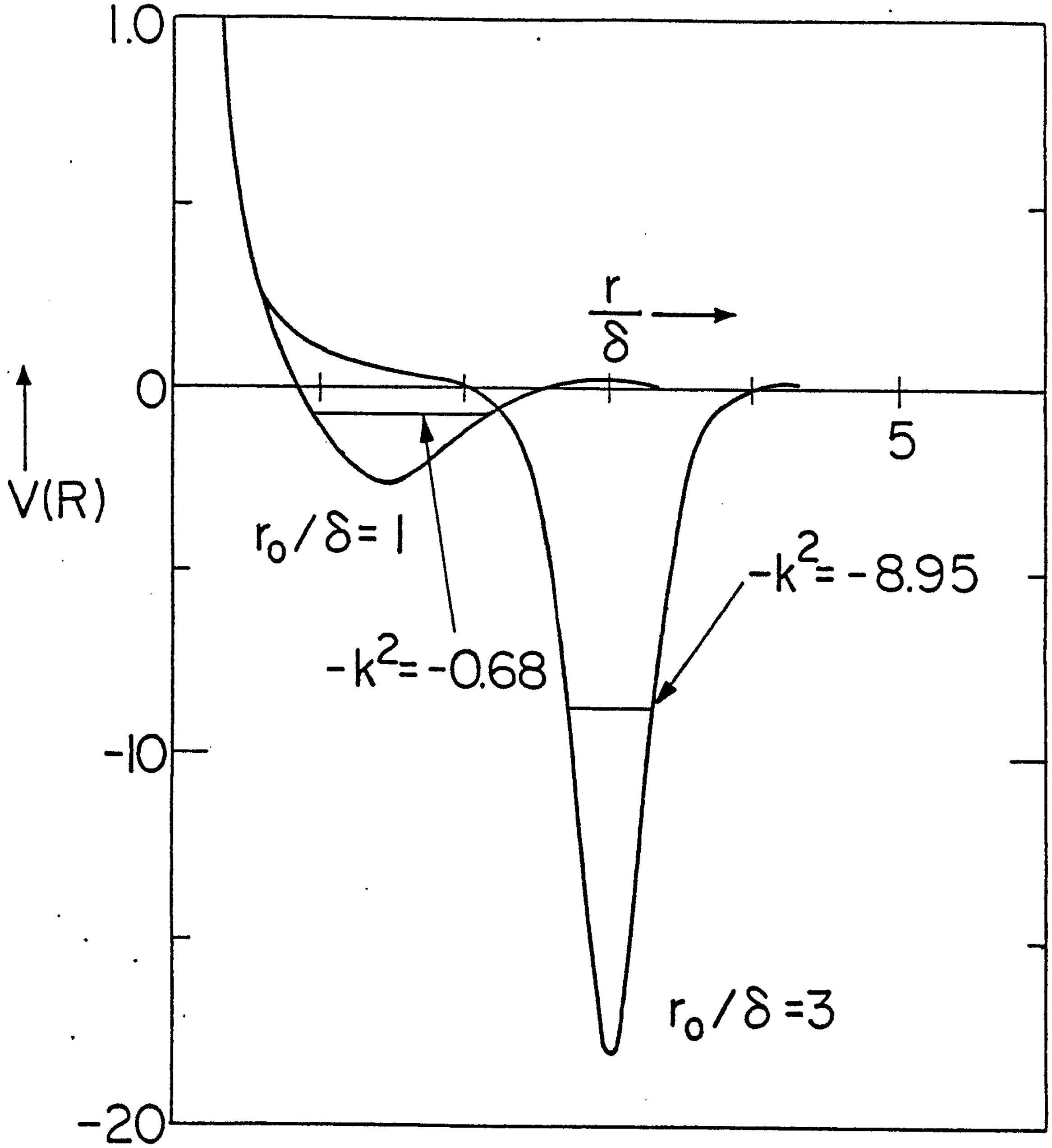

Fig. 1

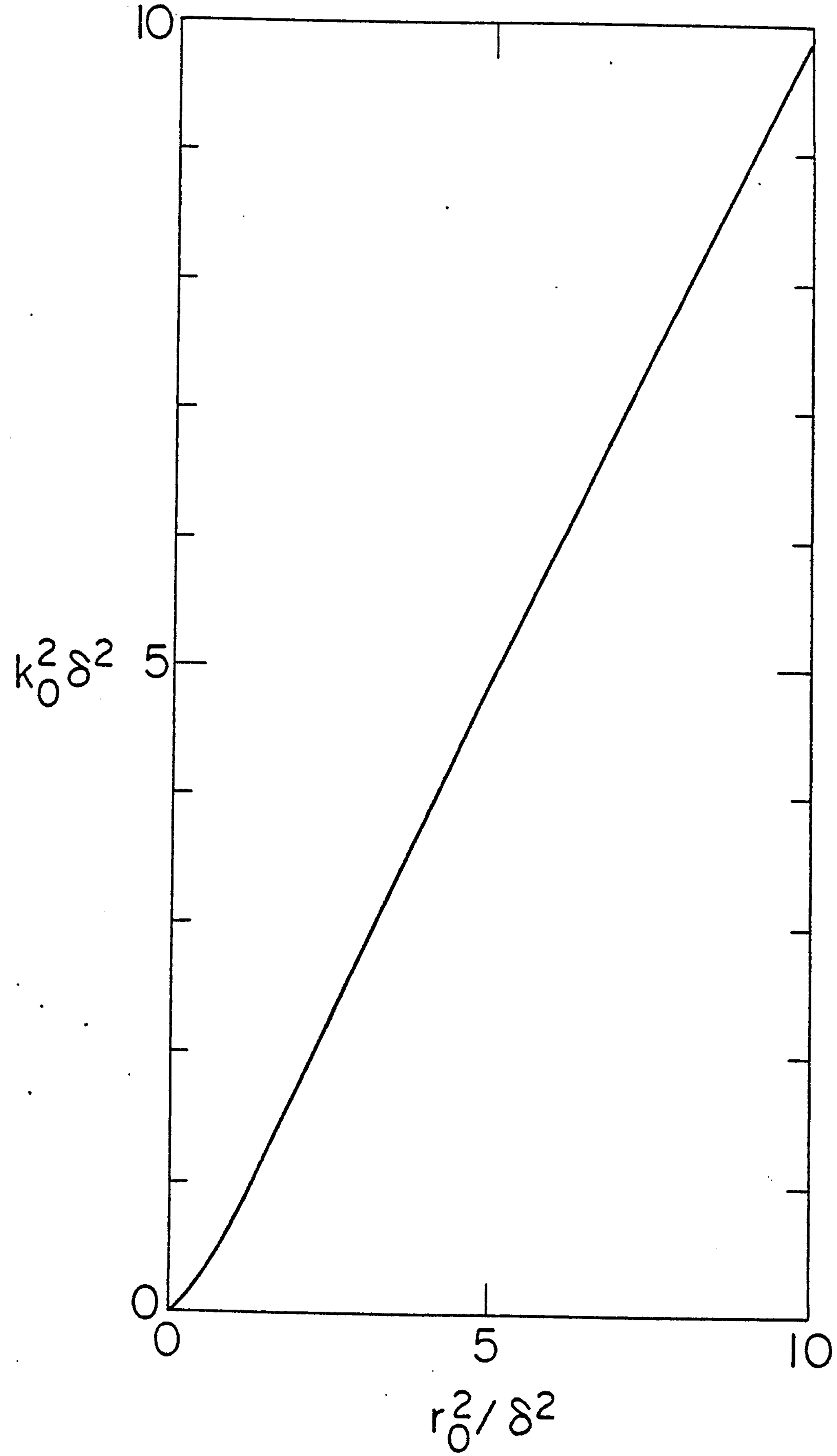

Fig. 2

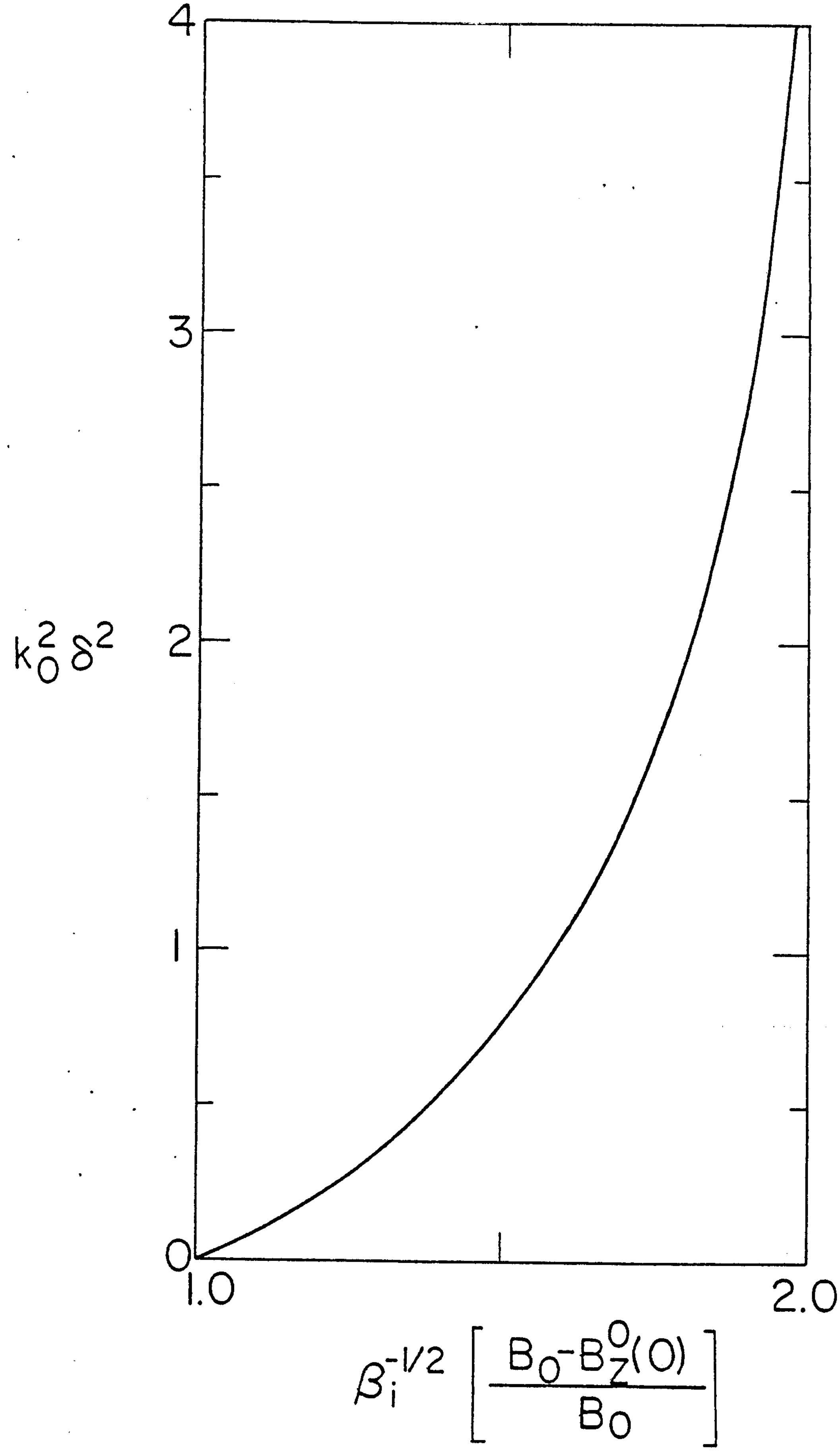

Fig. 3

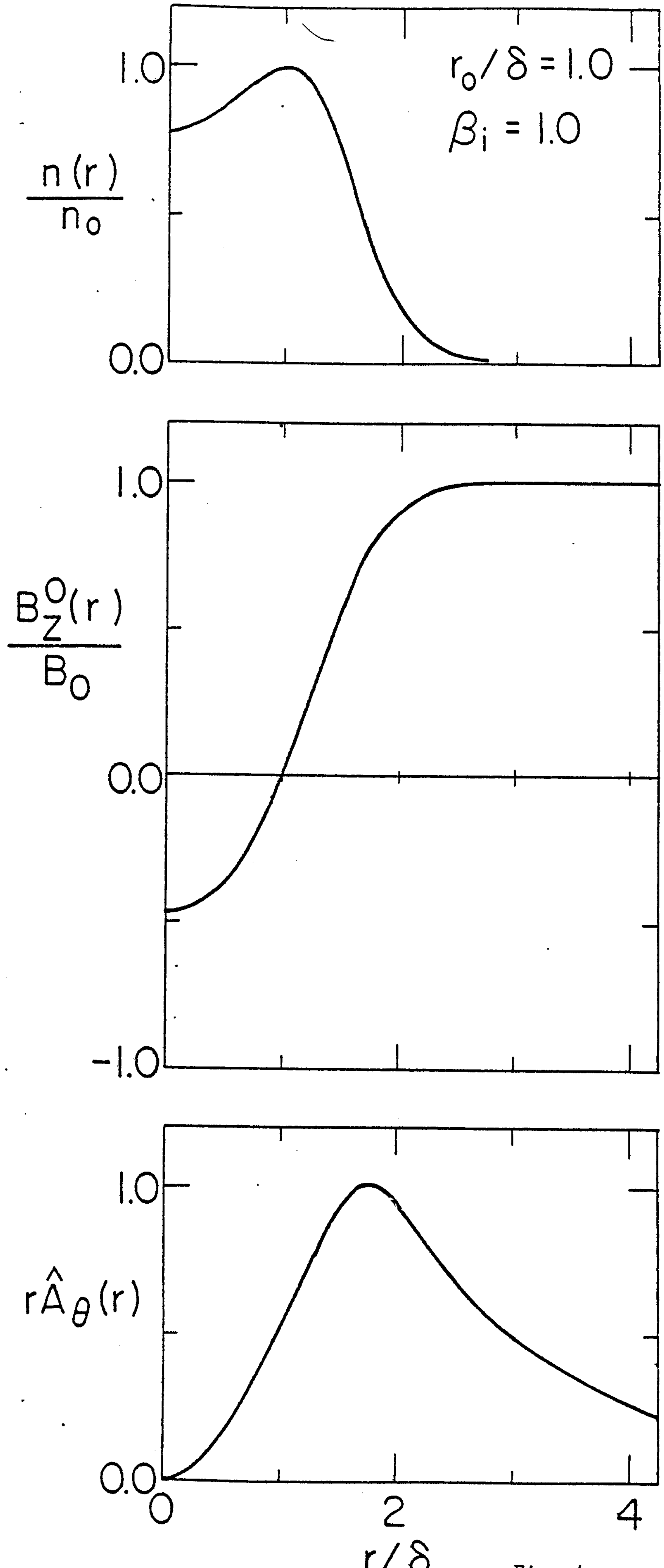
$r_o/\delta = 1.0$
$\beta_i = 1.0$
$\frac{n(r)}{n_o}$
$\frac{B_Z^0(r)}{B_0}$
$r\hat{A}_\theta(r)$
1.0
0.0
-1.0
0
2
4
r/δ

Fig. 4

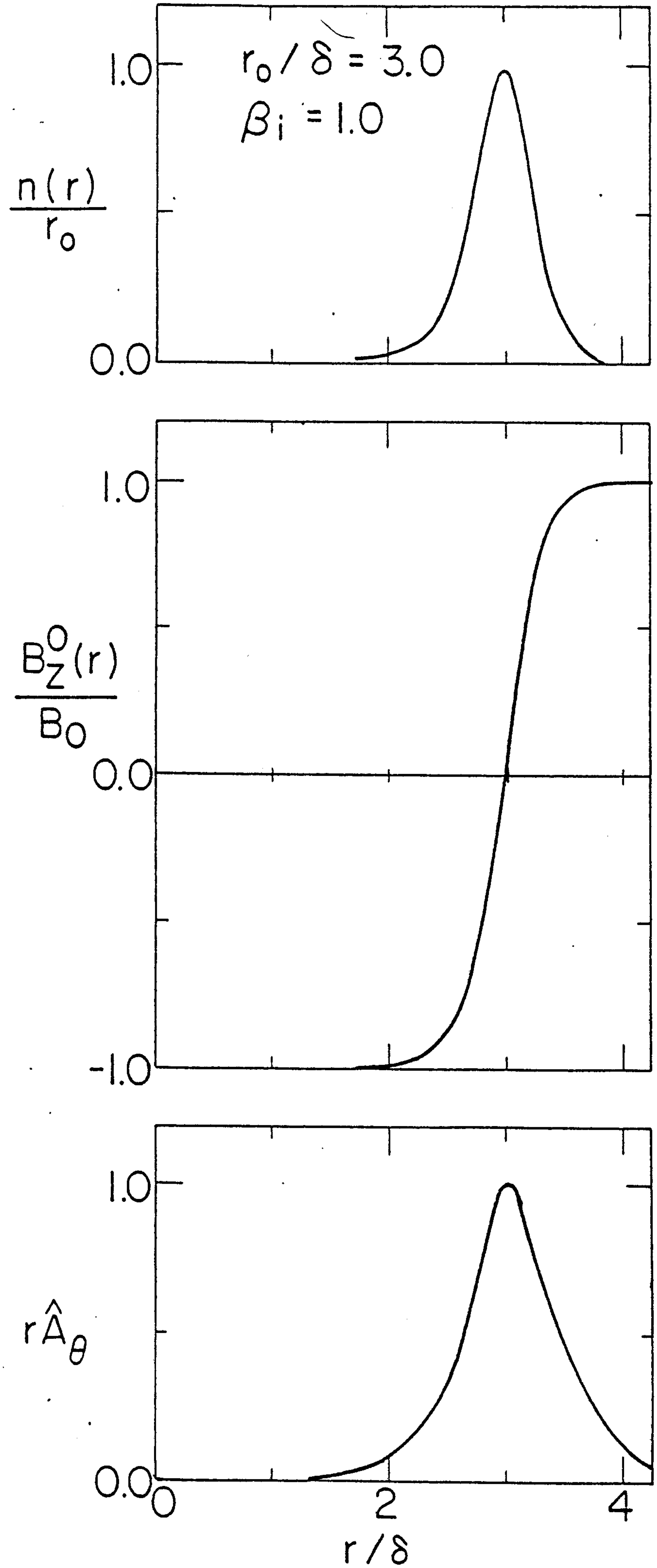
$r_o / \delta = 3.0$
$\beta_i = 1.0$
$\frac{n(r)}{r_o}$
1.0
0.0
$\frac{B_Z^O(r)}{B_O}$
1.0
0.0
-1.0
$r\hat{A}_\theta$
1.0
0.0
0
2
4
r/δ